



**HAL**  
open science

## Structural and dielectric study of the $\text{Na}_{0.5}\text{Bi}_{0.5}\text{TiO}_3\text{-PbTiO}_3$ and $\text{K}_{0.5}\text{Bi}_{0.5}\text{TiO}_3\text{-PbTiO}_3$ systems

Omar Elkechai, Pascal Marchet, Philippe Thomas, Michel Manier, Jean-Pierre Mercurio

► **To cite this version:**

Omar Elkechai, Pascal Marchet, Philippe Thomas, Michel Manier, Jean-Pierre Mercurio. Structural and dielectric study of the  $\text{Na}_{0.5}\text{Bi}_{0.5}\text{TiO}_3\text{-PbTiO}_3$  and  $\text{K}_{0.5}\text{Bi}_{0.5}\text{TiO}_3\text{-PbTiO}_3$  systems. *Journal of Materials Chemistry*, 1997, 7 (1), pp.91-97. 10.1039/a602148d . hal-02296080

**HAL Id: hal-02296080**

**<https://unilim.hal.science/hal-02296080>**

Submitted on 5 Jun 2020

**HAL** is a multi-disciplinary open access archive for the deposit and dissemination of scientific research documents, whether they are published or not. The documents may come from teaching and research institutions in France or abroad, or from public or private research centers.

L'archive ouverte pluridisciplinaire **HAL**, est destinée au dépôt et à la diffusion de documents scientifiques de niveau recherche, publiés ou non, émanant des établissements d'enseignement et de recherche français ou étrangers, des laboratoires publics ou privés.

## Structural and dielectric study of the $\text{Na}_{0.5}\text{Bi}_{0.5}\text{TiO}_3\text{--PbTiO}_3$ and $\text{K}_{0.5}\text{Bi}_{0.5}\text{TiO}_3\text{--PbTiO}_3$ systems

Omar Elkechai, Pascal Marchet, Philippe Thomas, Michel Manier and Jean-Pierre Mercurio\*  
Laboratoire de Matériaux Céramiques et Traitements de Surface, URA CNRS N° 320, Faculté des Sciences,  
123, Avenue Albert-Thomas, 87060 Limoges Cedex, France

### Abstract

A study of the  $\text{Na}_{0.5}\text{Bi}_{0.5}\text{TiO}_3\text{--PbTiO}_3$  and  $\text{K}_{0.5}\text{Bi}_{0.5}\text{TiO}_3\text{--PbTiO}_3$  systems has been carried out using X-ray diffraction, differential scanning calorimetry and dielectric measurements. The limits of the rhombohedral ( $\text{Na}_{0.5}\text{Bi}_{0.5}\text{TiO}_3$ -rich side) and tetragonal ( $\text{PbTiO}_3$ -rich side) solid solutions have been determined, as well as the evolution of their lattice parameters as a function of composition and temperature. Ceramic materials have been prepared by natural sintering (1090–1220 °C; 0.5 h) of powders obtained by solid-state reaction (900–1000°C; 20 h) of the corresponding oxides and carbonates. The dielectric permittivities of these materials have been measured in a wide frequency range for temperatures between 20 and 800 °C. The results showed that they all are ferroelectric at room temperature and exhibit either a diffuse, probably second-order phase transition, or a sharp, first order-like phase transition from the ferroelectric to the paraelectric state, depending on the composition.

Lead titanate–zirconate ceramics (PZT) are currently the most used ferroelectric materials in the field of piezoelectric applications. A noticeable feature of these materials is the occurrence of a morphotropic phase boundary (MPB) in the phase diagram which separates tetragonal and rhombohedral ferroelectric regions. Solid solutions with compositions close to the MPB present the best electromechanical properties. In the research of new complex systems with interesting piezoelectric characteristics, care should be taken that thermal and time stability of the properties is connected with the value of the Curie temperature of the components. Previous works have shown that in most cases this corresponds to the situation where the MPB is located between tetragonal and rhombohedral phases.<sup>1</sup>

Up to now, results concerning systems other than PZTs have only been devoted to either  $\text{Na}_{0.5}\text{Bi}_{0.5}\text{TiO}_3\text{--}(\text{Sr},\text{Ba})\text{TiO}_3$  or the low-lead range of  $\text{Na}_{0.5}\text{Bi}_{0.5}\text{TiO}_3\text{--PbTiO}_3$ .<sup>2–6</sup> A study was therefore conducted on the whole  $\text{Na}_{0.5}\text{Bi}_{0.5}\text{TiO}_3\text{--PbTiO}_3$  (NBT–PT) and  $\text{K}_{0.5}\text{Bi}_{0.5}\text{TiO}_3\text{--PbTiO}_3$  (KBT–PT) systems, which are both likely to present MPBs. Actually, at room temperature NBT is rhombohedral ( $T_c \approx 320$  °C), KBT is tetragonal ( $T_c \approx 380$  °C) as is PT ( $T_c \approx 490$  °C).<sup>7</sup> This paper presents the results concerning the preparation of some materials belonging to this family as well as their thermal and dielectric properties.

### Experimental

Polycrystalline compounds were prepared by solid-state reaction of the corresponding oxides or carbonates. Stoichiometric mixtures of reagent grade  $\text{TiO}_2$ ,  $\text{Bi}_2\text{O}_3$ ,  $\text{Na}_2\text{CO}_3$ ,  $\text{K}_2\text{CO}_3$  and  $\text{PbO}$  (or  $\text{PbCO}_3$ ) were mixed thoroughly and calcined in alumina crucibles between 900 and 1000°C for 20 h. Further calcinations were necessary to achieve complete reaction. Phase characterisation and phase boundary limits were determined by X-ray diffraction (XRD) with a Siemens D5000 diffractometer (graphite monochromator, Cu-K $\alpha$  radiation). The lattice parameters were refined by a least-squares method. The structural evolution of the compounds with temperature was observed using a high-temperature X-ray (HTXRD) attachment (Anton Parr HTK10) working between room temperature and 1000°C. Differential scanning calorimetry (DSC) analyses were performed in air using a Netzsch STA 409 DSC device.

The powders were pressed into discs of diameter 10 mm and thickness 1 mm and were sintered in air at 1090–1220 °C, depending on the composition. The thermal cycle consisted of heating at 5 °C min<sup>-1</sup> to the highest temperature (dwelling time 30 min) followed by natural cooling to room temperature in the oven. Samples with 90–95% of the theoretical density were obtained. After polishing the major faces, they were coated with a low-temperature silver or gold paste fired at 600°C for 10 min, aged overnight at 100 °C and left for 24 hours at room temperature before the measurements. Low-frequency dielectric measurements were carried out between room temperature and 1000°C (at increasing and decreasing temperature) at chosen frequencies in the range

### Results

#### Structural characterisation

At room temperature, NBT is rhombohedral ( $a = 0.3891$  nm,  $\alpha = 89.6^\circ$ ) whereas KBT and PT are tetragonal with the following lattice parameters; KBT,  $a = 0.3918$  nm,  $c = 0.3996$  nm; PT,  $a = 0.3899$  nm,  $c = 0.4155$  nm.

### NBT–PT system

XRD data showed two  $(\text{Na}_{0.5}\text{Bi}_{0.5})_{1-x}\text{Pb}_x\text{TiO}_3$  solid solution ranges; rhombohedral on the sodium-rich side and tetragonal on the lead-rich side, separated by a biphasic region for  $0.10 < x < 0.18$ . This result is somewhat different from that obtained by Takenaka et al. and recently by Park and Hong, who did not find a biphasic range, but found a morphotropic phase boundary at  $x = 0.13\text{--}0.14$  between rhombohedral and tetragonal symmetry at room temperature.<sup>4,6</sup> The observed discrepancy of the present results with respect to other works could be attributed to the different preparation processes, especially the annealing conditions. Fig. 1 shows the evolution of the room-temperature lattice parameters as a function of the composition as well as the  $c/a$  ratio within the tetragonal range. As expected, they increase with  $x$  according to the increase of the mean ionic radii which change from 0.134 nm (Na,Bi) to 0.147 nm (Pb). Nevertheless, in the tetragonal region, the  $c$  parameter increases more strongly than  $a$ , leading to a change of the tetragonality from 1.02 ( $x = 0.18$ ) to 1.06 ( $x = 1$ ). This result is slightly different from the parent system NBT–KBT in which the tetragonal distortion does not vary greatly with the composition within the tetragonal domain.<sup>8</sup>

Variation-temperature XRD experiments were performed on several samples belonging to both single-phase domains (rhombohedral and tetragonal) up to temperatures well above the Curie temperature. The thermal evolution of lattice parameters and volume for  $\text{Na}_{0.5}\text{Bi}_{0.5}\text{TiO}_3$  and  $(\text{Na}_{0.5}\text{Bi}_{0.5})_{1-x}\text{Pb}_x\text{TiO}_3$  ( $x=0.03, 0.05$  and  $0.09$ ) are presented in Fig. 2 as examples of rhombohedral solid solutions. In the temperature range studied, the parameters show a very slight monotonic increase with increasing temperature, and there are no anomalies at temperatures close to the expected structural phase transitions. This is because the low-temperature rhombohedral unit cell is not strongly distorted with respect to the prototype high-temperature cubic cell. This result is similar to that observed previously in the NBT–KBT system.<sup>8</sup>

Fig. 3 shows the thermal evolution of the lattice parameters of tetragonal  $(\text{Na}_{0.5}\text{Bi}_{0.5})_{1-x}\text{Pb}_x\text{TiO}_3$  solid solutions with  $x = 0.30, 0.50, 0.70$  and  $1$ . In each case, increasing temperature causes the tetragonal lattice parameters to vary in opposite senses: i.e. up to the transition temperature  $a$  increases and  $c$  decreases almost monotonously. Nevertheless, the way in which the parameters change between room temperature and the transition temperature is dependent on the composition. On the left-hand side of the tetragonal domain,  $a$  and  $c$  reach almost the same value corresponding to the cubic lattice parameter at the transition temperature as shown in Fig. 3 (left-hand side). On the right-hand (PbTiO<sub>3</sub>-rich) side the thermal variation of the lattice parameters at the transition shows a strong discontinuity, which is clearly visible when the lead content is higher than  $0.5$ .

### KBT–PT system

As expected, XRD data showed that KBT and PT give rise to a full range solid solution with tetragonal and PT give rise to a full range solid solution with tetragonal symmetry. The evolution of the room-temperature lattice parameters of  $(\text{Na}_{0.5}\text{Bi}_{0.5})_{1-x}\text{Pb}_x\text{TiO}_3$  solid solutions as a function of composition is given in Fig. 4. As Pb is substituted for (Na,Bi), the  $a$  parameter of the tetragonal cell decreases slightly but the  $c$  parameter increases strongly, both quasi-linearly, leading to a more and more distorted unit cell: the tetragonality,  $c/a$ , changes from 1.02 (KBT) to 1.06 (PT). The thermal evolution of the lattice parameters of some selected compositions of the system are given in Fig. 5. The behaviour is similar to that observed for the tetragonal solid solutions of the NBT–PT system; the higher the lead content the steeper the discontinuity of the lattice parameters (cf. Fig. 3).

### Dielectric properties

The dielectric properties of the ceramic materials were measured at several frequencies between 1 kHz and 10 MHz. In general, the results showed no significant frequency dispersion of either dielectric permittivity or loss. For clarity, only the results obtained at 1 MHz will be given hereafter.

### NBT–PT system

The thermal variations of the dielectric permittivities and losses at 1 MHz of some compositions of the NBT–PT system are given in Fig. 6A ( $x=0, 0.03, 0.08$  and  $0.09$ —rhombohedral) and B ( $x=0.19, 0.20, 0.30$  and  $0.60$  tetragonal). They clearly show different behaviour according to the symmetry: rhombohedral low-lead content materials exhibit a diffuse character whereas a sharp evolution of the permittivity is present in tetragonal lead-rich materials. The rhombohedral solid solutions exhibit the same behaviour as similar materials in the NBT–KBT system.<sup>8</sup> The temperature of the maximum permittivity is lower than that for pure NBT, but is almost composition independent along the rhombohedral range. In the tetragonal range, the sharpness of the permittivity maximum becomes more and more pronounced as the lead content is increased.

### KBT–PT system

In contrast to the previous system, KBT–PT does not exhibit any lack of miscibility over the whole composition range. As a consequence, one expects that the dielectric properties, especially the thermal variations of the dielectric permittivities, will have continuous behaviour from KBT to PT. Fig. 7 shows the thermal variations of the dielectric permittivities and losses at 1 MHz of compositions within the KBT–PT system. As observed

already for the tetragonal compositions of the NBT–PT system, the curves  $\varepsilon(T)$  show a progressive evolution from a diffuse maximum (KBT) to a very sharp one (PT).

## Discussion

The dielectric permittivities of NBT and KBT exhibit broad maxima at 320 and 380 °C respectively, undoubtedly connected with the transition towards the cubic paraelectric state.<sup>7</sup> In contrast, PT is known to present a sharp permittivity maximum at 490°C. As the compositions at the extremes of the systems under investigation show well established ferroelectric behaviour at room temperature, the discussion of the thermal evolution of the structural and dielectric characteristics over the whole composition ranges will be conducted in terms of the phenomenological approach developed by Devonshire after the Ginzburg–Landau theory of phase transitions.<sup>9</sup> A main consequence of this theory is that the thermodynamical nature of the phase transition of a ferroelectric material can be derived qualitatively from the evolution of the reciprocal permittivity below and above the transition temperature,  $T_t$ . For a so-called first-order phase transition, the ratio  $r$  of the slopes of the reciprocal permittivities,  $\varepsilon^{-1}(T < T_t) / \varepsilon^{-1}(T > T_t)$ , should be *ca.* 4, whereas it should be only 2 for a second-order phase transition. In addition, for a second-order phase transition, the Curie temperature is very close to the temperature,  $T_0$ , extrapolated from the high temperature variations of  $\varepsilon^{-1}$ , whereas this extrapolation always leads to a  $T_0$  value less than  $T_c$  for a first-order phase transition. The overall properties of the materials under investigation are strongly dependent on their crystal structures, either rhombohedral for the (Na,Bi)-rich side of NBT–PT, or tetragonal for both the lead-rich side of NBT–PT and the whole composition range of KBT–PT. The discussion will be focused separately on the properties of materials with (i) rhombohedral and (ii) tetragonal structures.

### (i) Rhombohedral solid solutions: $(\text{Na}_{0.5}\text{Bi}_{0.5})_{1-x}\text{Pb}_x\text{TiO}_3$ ( $0 < x \leq 0.09$ )

A careful examination of the thermal evolutions of the permittivities show a composition dependent weak shoulder on the low-temperature side of the peak. In NBT, this shoulder was assigned initially to a ferroelectric–antiferroelectric transition.<sup>2</sup> Recently, Park and Hong refined this sequence and proposed a diffuse phase transition zone in the temperature range 240–280 °C for  $x < 0.1$ .<sup>6</sup> In the present work, the temperatures at which this shoulder appears decreases from *ca.* 230 °C for NBT to *ca.* 150 °C for the upper limit of the rhombohedral domain. This result is similar to that already observed for NBT–ST solid solutions where the ferroelectric–antiferroelectric transition temperature decreases monotonically as the strontium content increases.<sup>5</sup> As a consequence, Devonshire calculations cannot be applied to the low-temperature side of the permittivity peak.

### (ii) Tetragonal solid solutions: $(\text{Na}_{0.5}\text{Bi}_{0.5})_{1-x}\text{Pb}_x\text{TiO}_3$ ( $0.18 < x \leq 1$ ) and $(\text{K}_{0.5}\text{Bi}_{0.5})_{1-x}\text{Pb}_x\text{TiO}_3$ ( $0 \leq x \leq 1$ )

These tetragonal solid solutions show similar behaviour. The phenomenological calculation can be carried out successfully over the whole solubility range for NBT–PT and for  $x > 0.20$  in the case of KBT–PT. The Curie constants calculated at high temperature are in the range  $2\text{--}2.5 \times 10^5$  K, as observed commonly for one-dimensional ferroelectrics (e.g. perovskites, tungsten bronzes). When the lead content increases to PT the thermal variations of the permittivities change gradually from a diffuse to a non-diffuse character (Fig. 6B and 7), as do the slope ratios  $r$  of the reciprocal permittivities which change from 2.5 to 4 (Fig. 8). After Devonshire, this behaviour should correspond to a progressive evolution from a diffuse, second-order to a sharp, first-order phase transition as the compositions approaches PT. This assumption should be supported by the thermal evolution of the lattice parameters. At low lead contents, the transition from the tetragonal to the cubic symmetry occurs gradually by a mere convergence of the lattice parameters  $a$  and  $c$  towards the value of the parameter of the cubic unit cell at the transition temperature. So, there is no volume change at the transition. However, for  $x > 0.40$ , there is a discontinuous change of symmetry at the transition temperature leading to an increase in cell volume. This change becomes larger as  $x$  increases. The volume variation, which changes from  $-0.07 \times 10^{-3}$  (NBT–PT) to  $-0.4 \times 10^{-3}$  nm<sup>3</sup> (PT), is characteristic of a first-order phase transition. In addition, DSC experiments carried out at increasing and decreasing temperatures have shown very well defined peaks corresponding to the transition temperatures. With a heating/cooling rate of 20 °C min<sup>-1</sup>, the DSC curves exhibit thermal peaks at the transition temperatures with a thermal hysteresis  $\Delta T \approx -15$  °C, as observed already in pure PT. These peaks are even stronger and sharper when the lead content is increased. The energy involved in the phase transitions can be calculated accurately only for compositions where  $x > 0.30$ . These calculations show that the energies increase linearly up to  $x = 0.70$  and then increase more rapidly as  $x$  approaches unity. This behaviour is very similar to that of the increase in volume change at the transition calculated from the lattice parameters.

In the tetragonal domain, the more striking feature is the evolution of the temperature of the phase transition from tetragonal to cubic symmetry. As the tetragonal compositions seem to behave as regular solid solutions (e.g. KBT–PT solid solutions follow Vegard’s law), one expects a linear variation of the Curie temperatures as observed, for example, in BT–ST or BT–PT. However, in both cases, the Curie temperatures show a maximum value at *ca.* 70–80 mol% lead, in close agreement with HTXRD and DSC experiments (Fig. 9). This unusual behaviour could be connected with the respective polarizabilities of lead and (Na,Bi) or (K,Bi). Up to *ca.* 60 mol% lead, the influence of increasing lead content dominates over the effect of decreasing the (Na,Bi) or (K,Bi) content and the Curie

temperature increases, whereas above 60 mol% lead, the decrease of (Na,Bi) or (K,Bi) content is not compensated by the increase in Pb content and the Curie temperature decreases to that of PT.

### **Conclusion**

Ferroelectric to paraelectric phase transitions in the NBT–PT and KBT–PT systems were studied as a function of composition and temperature. The nature of the transition was discussed in terms of the phenomenological derivation of the Ginzburg–Landau theory. The diffuse character decreases strongly as the lead content increases in both systems. A study of the thermal evolution of the polarisation coupled with variable-temperature optical microscopy examinations of these materials is now in progress in order to confirm the above statements.

### **References**

- 1 B. Jaffe, W. R. Cook and H. Jaffe, *Piezoelectric Ceramics*, Academic Press, London, 1971.
- 2 B. Vakhrushev, V. A. Isupov, B. E. Kvyatkovsky, N. M. Okuneva, I. P. Pronin, G. A. Smolenskii and P. P. Syrnikov, *Ferroelectrics*, 1985, 63, 153.
- 3 C. S. Tu, I. G. Siny and V.H. Schmidt, *Phys. Rev. B*, 1994, 49, 11550.
- 4 T. Takenaka, K. Sakata and K. Toda, *Ferroelectrics*, 1990, 106, 375.
- 5 K. Sakata and Y. Masuda, *Ferroelectrics*, 1974, 7, 347.
- 6 S-E. Park and K. S. Hong, *J. Appl. Phys.*, 1996, 79, 383.
- 7 G. A. Smolenskii, V. A. Isupov, A. I. Agranovskaia and N. N. Krainik, *Fiz. Tverdogo Tela*, 1960, 2, 2982.
- 8 O. Elkechai, M. Manier and J. P. Mercurio, *Phys. Status Solidi A*, in the press.
- 9 A. F. Devonshire, *Philos. Mag.*, 1949, 40, 1040.

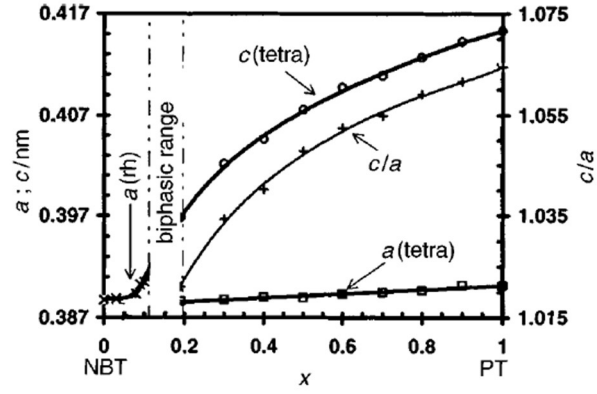


Fig. 1 NBT-PT system. Room-temperature lattice parameters vs. composition.

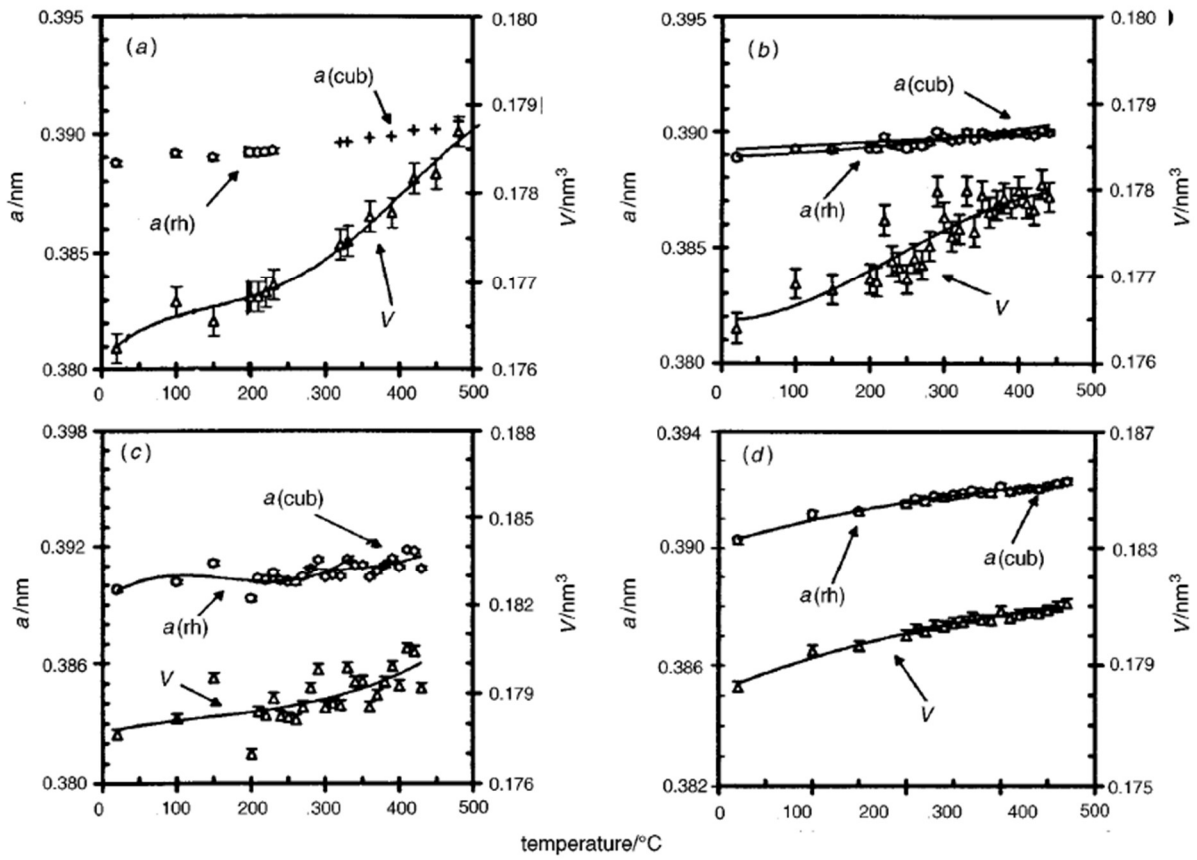


Fig. 2 NBT-PT system: rhombohedral range. Lattice parameters and cell volume vs. temperature for  $(\text{Na}_{0.5}\text{Bi}_{0.5})_{1-x}\text{Pb}_x\text{TiO}_3$ :  $x = 0$  (a), 0.03 (b), 0.05 (c) and 0.09 (d).

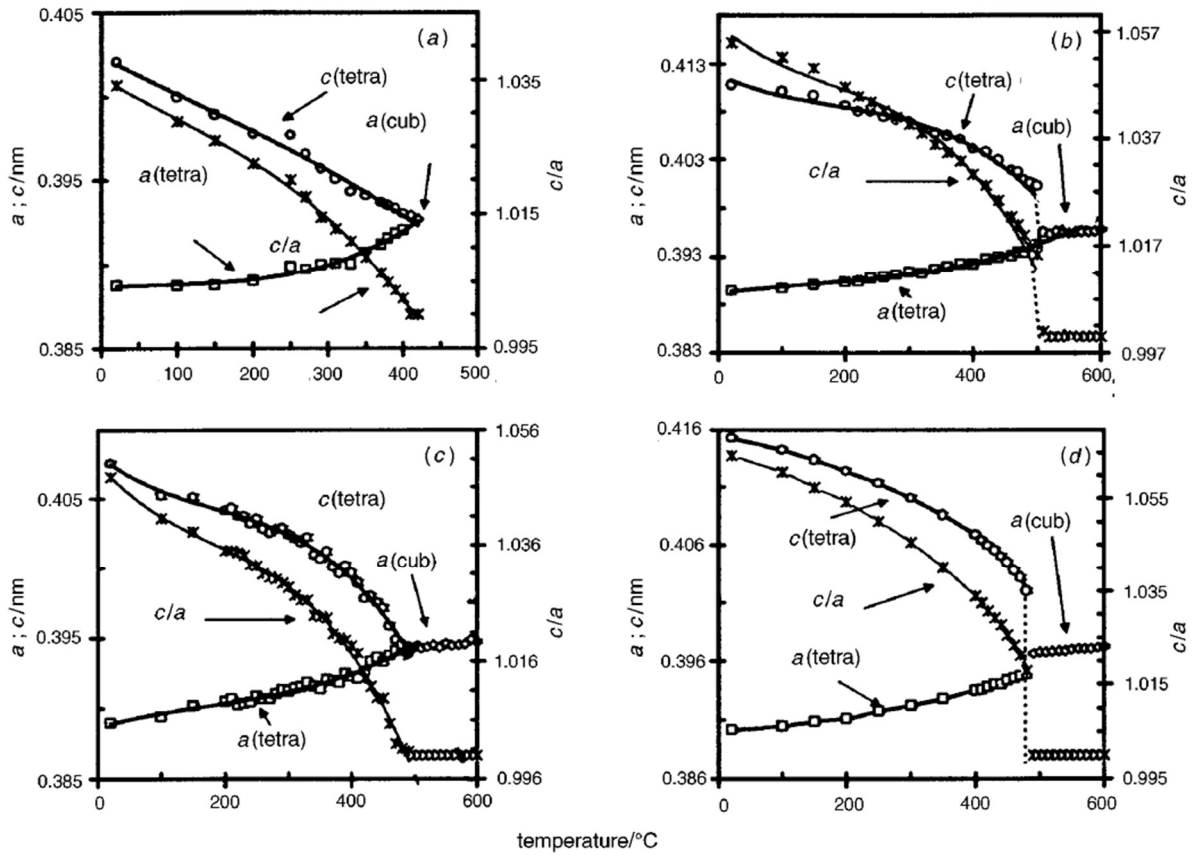


Fig. 3 NBT-PT system: tetragonal range. Lattice parameters and cell volume vs. temperature for  $(\text{Na}_{0.5}\text{Bi}_{0.5})_{1-x}\text{Pb}_x\text{TiO}_3$ ;  $x = 0.30$  (a), 0.50 (b), 0.70 (c) and 1 (d).

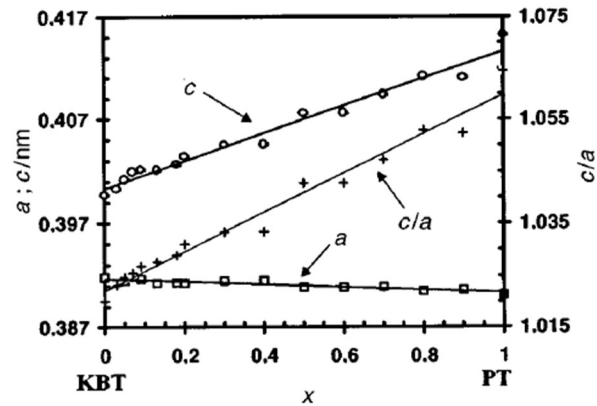


Fig. 4 KBT-PT system. Room-temperature lattice parameters vs. composition.

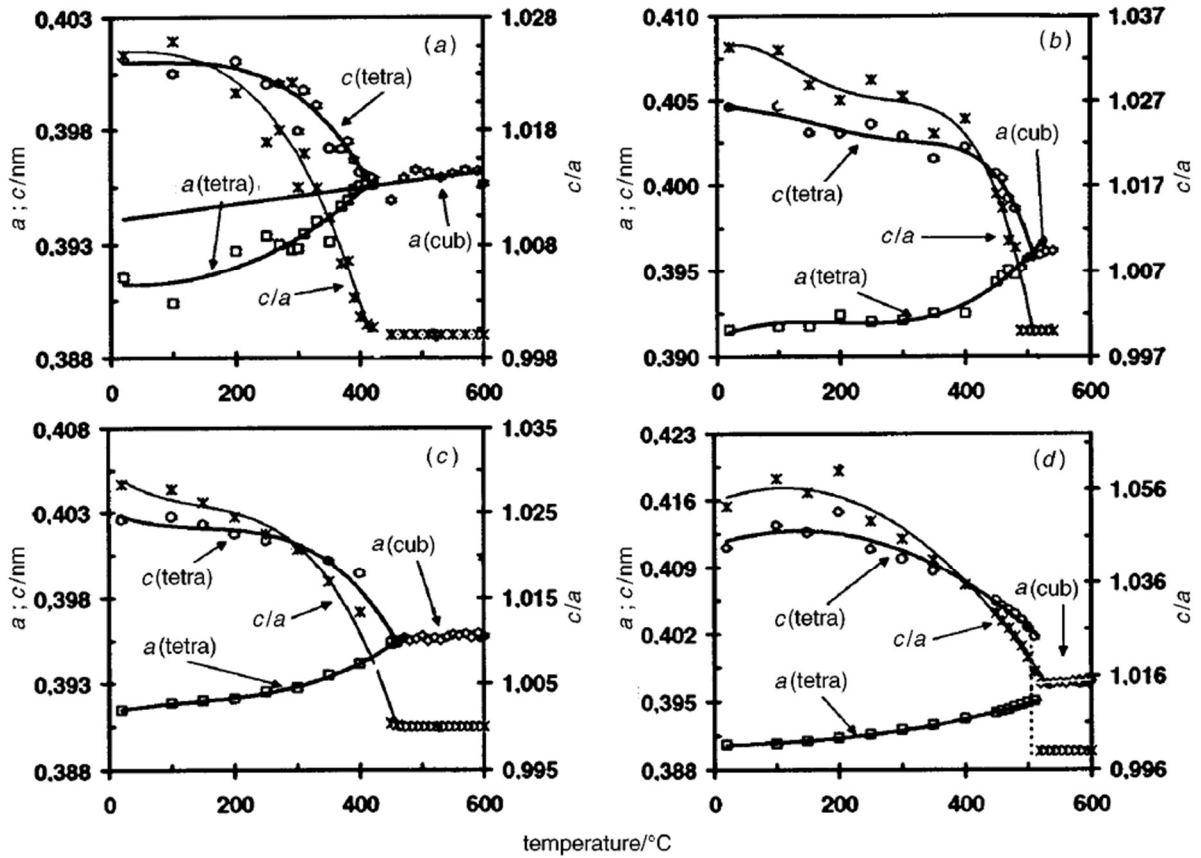


Fig. 5 KBT-PT system. Lattice parameters vs. temperature for  $(K_{0.5}Bi_{0.5})_{1-x}Pb_xTiO_3$ :  $x = 0.05$  (a),  $0.20$  (b),  $0.40$  (c) and  $0.90$  (d).

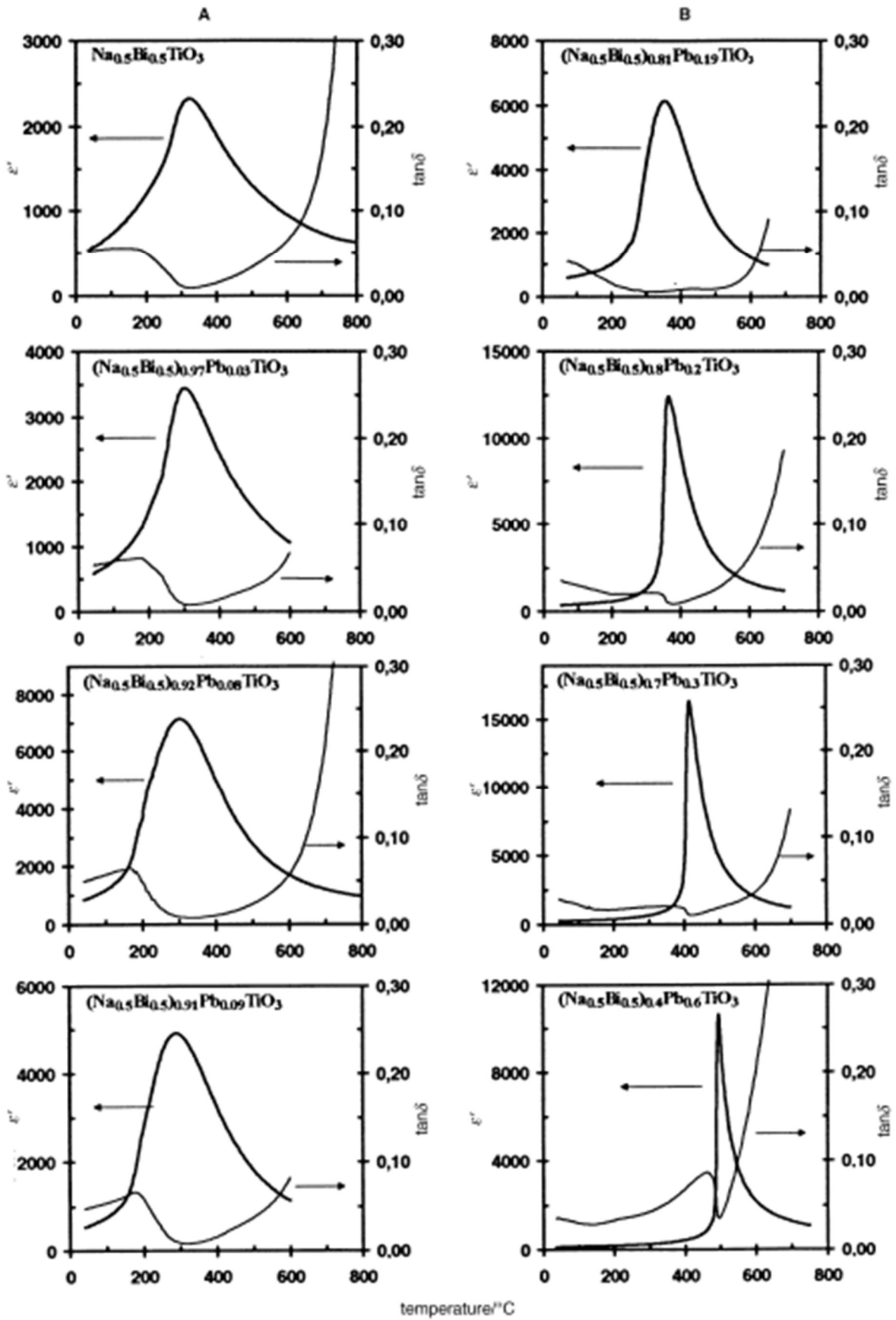


Fig. 6 NBT-PT system. Permittivity and loss vs. temperature for  $(\text{Na}_{0.5}\text{Bi}_{0.5})_{1-x}\text{Pb}_x\text{TiO}_3$ . A, rhomboidal range:  $x = 0$  (a), 0.03 (b), 0.08(c) and 0.09 (d). B, tetragonal range:  $x = 0.19$  (a), 0.20 (b), 0.30 (c) and 0.60 (d).

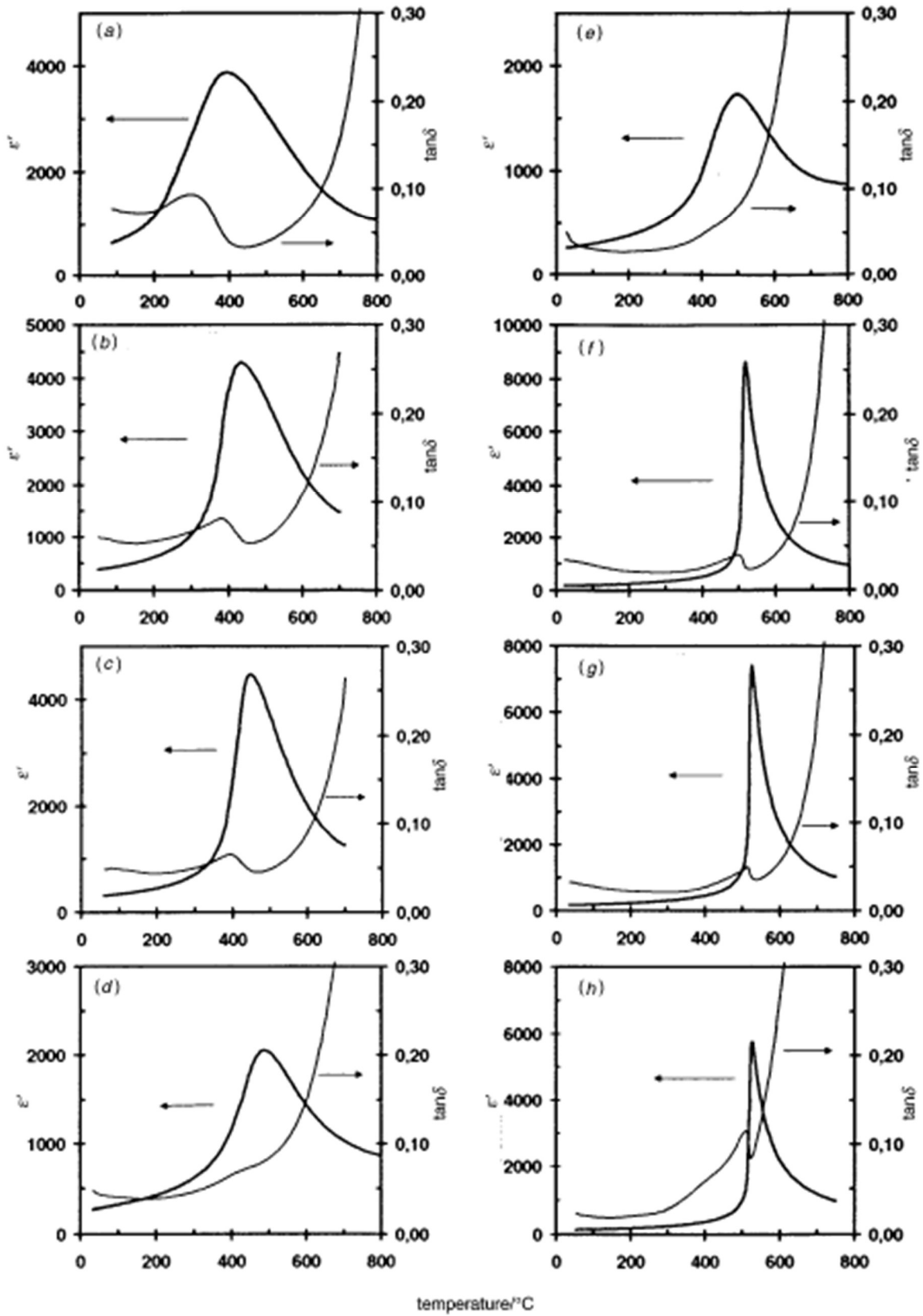
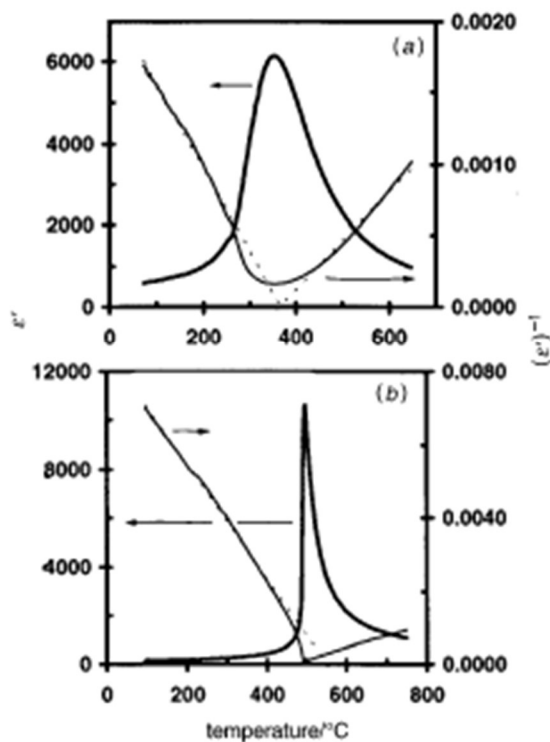
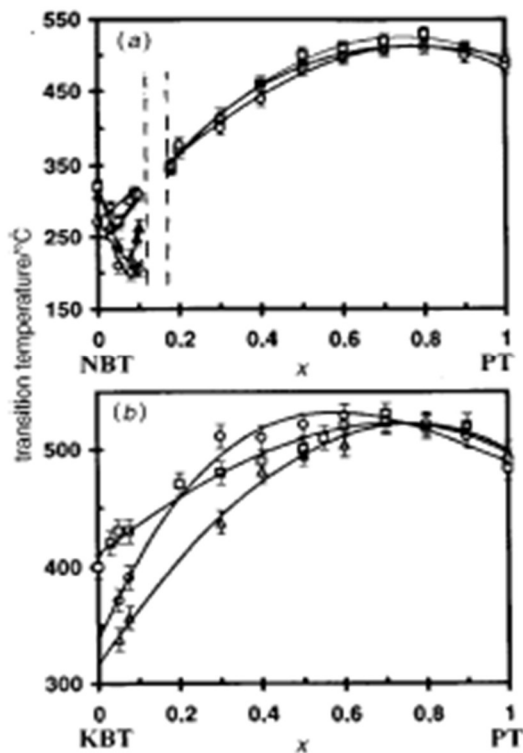


Fig. 7 KBT-PT system. Permittivity and loss vs. temperature for  $(K_{0.5}Bi_{0.5})_{0.5-1-x}Pb_xTiO_3$ :  $x = 0$  (a), 0.09 (b), 0.18 (c), 0.30 (d), 0.40 (e), 0.50 (f), 0.60 (g) and 0.80 (h).



**Fig. 8** Direct and reciprocal permittivities of two selected NBT-PT solid solutions showing (a) second-order ( $x = 0.19$ ) and (b) first-order ( $x = 0.60$ ) phase transitions



**Fig. 9** Transition temperatures vs. composition from HTXRD ( $\square$ , increasing T) and DSC ( $\Delta$ , increasing T ;  $\circ$ , decreasing T) for (a) NBT-PT and (b) KBT-PT